Bioelectromagnetics 20:399–413 (1999)

Residential Magnetic Fields Predicted From Wiring Configurations: I. Exposure Model

Joseph D. Bowman,[1]* Duncan C. Thomas,[2] Liangzhong Jiang,[2] Feng Jiang,[2] and John M. Peters[2]

[1]*National Institute for Occupational Safety and Health, Cincinnati, Ohio*
[2]*Department of Preventive Medicine, University of Southern California, Los Angeles, California*

A physically based model for residential magnetic fields from electric transmission and distribution wiring was developed to reanalyze the Los Angeles study of childhood leukemia by London et al. For this exposure model, magnetic field measurements were fitted to a function of wire configuration attributes that was derived from a multipole expansion of the Law of Biot and Savart. The model parameters were determined by nonlinear regression techniques, using wiring data, distances, and the geometric mean of the ELF magnetic field magnitude from 24-h bedroom measurements taken at 288 homes during the epidemiologic study. The best fit to the measurement data was obtained with separate models for the two major utilities serving Los Angeles County. This model's predictions produced a correlation of 0.40 with the measured fields, an improvement on the 0.27 correlation obtained with the Wertheimer-Leeper (WL) wire code. For the leukemia risk analysis in a companion paper, the regression model predicts exposures to the 24-h geometric mean of the ELF magnetic fields in Los Angeles homes where only wiring data and distances have been obtained. Since these input parameters for the exposure model usually do not change for many years, the predicted magnetic fields will be stable over long time periods, just like the WL code. If the geometric mean is not the exposure metric associated with cancer, this regression technique could be used to estimate long-term exposures to temporal variability metrics and other characteristics of the ELF magnetic field which may be cancer risk factors. Bioelectromagnetics 20:399–413, 1999.

Key words: ELF magnetic fields; wire codes; childhood leukemia

INTRODUCTION

In their landmark study of childhood leukemia, Wertheimer and Leeper [1979] devised their ''wire code'' for predicting residential magnetic fields from the wiring configurations of electric transmission and distribution lines in the immediate vicinity of a child's home. In its most common form, the Wertheimer-Leeper (WL) code uses distances from the electric lines to the home and selected wiring parameters to assign the residence to one of five categories, which represent household exposures to extra low frequency (ELF) magnetic fields [Wertheimer and Leeper, 1982]. In studies of the WL code for U.S. residences, magnetic field magnitudes do have an upward gradient across categories, but the spread in the measurements within categories is even greater [Kheifets et al., 1997]. Moreover, the correlation between the WL code and magnetic field measurements is low ($r = 0.27$ in the Los Angeles data set that we will consider).

Although the WL code is a crude predictor of residential magnetic fields, it has been associated with childhood leukemia risks in three studies [Wertheimer and Leeper, 1979; Savitz et al., 1988; London et al., 1991], but not in two others [Fulton et al., 1980; Linet et al., 1997]. This ''wire code paradox'' has become a central issue in the debate over the possible health effects of magnetic fields [National Research Council, 1996; Kheifets et al., 1997]. One possible explanation is that the ELF magnetic field magnitude may indeed be the exposure metric causing the cancers, but associations between measurements and leukemia risk have been severely attenuated by the field's great variability over space and time. Because wiring

Contract grant sponsor: Electric Power Research Institute. Contract grant number: 2964 1; Contract grant sponsors: Los Angeles Dept. of Water and Power; Southern California Edison.

*Correspondence to: Joseph D. Bowman, National Institute for Occupational Safety and Health, 4676 Columbia Parkway, Cincinnati, OH 45266. E-mail: jdb0@cdc.gov

Received for review 8 July 1997; Final revision received 7 December 1998

configurations do not change as rapidly over time as magnetic field magnitudes, the WL code, therefore, may be a better measure of long-term exposure.

An opportunity to test whether the long-term average magnetic field may be the causal agent is provided by additional wire configuration data collected during the Los Angeles case-control study of childhood leukemia [London et al., 1991]. From the beginning of this study, observers doubted whether the WL code would make good predictions of magnetic fields in Los Angeles County. Those utilities often have ''delta-connected'' distribution lines with no neutral wires, which differs fundamentally from wiring practices in Denver, Colorado, where the WL code was devised. After surveying magnetic fields in Los Angeles neighborhoods, Leeper [1986–1989] commented: ''Our coding system simply doesn't tell you what to do with delta connected primaries!'' Furthermore, the Seattle, Washington, study by Kaune et al. [1987] had shown that predictions better than the WL code could be obtained in their region by regression modeling with magnetic field measurements and wire configuration data. To obtain similar improvements in magnetic field predictions, the Los Angeles study also collected substantial wire configuration data, far beyond that needed for the WL code.

In this paper, we use this wire configuration data to develop a quantitative model of the long-term magnetic field exposures. The basic approach is to use the detailed wiring information and the magnetic field measurements, together with fundamental physical principles, to build a regression model that should predict residential exposures more accurately than the WL code. In a companion paper [Thomas et al., 1999], the magnetic field exposures from the model are used to reanalyze the childhood leukemia risks.

THEORY

To predict residential magnetic fields, we first derive an equation from the laws of electromagnetism that can be used for regression modeling with wiring configurations and measurements. Magnetic fields are vector functions of space and time produced by electric current flowing in a wire, which is described by the Law of Biot and Savart [Lorrain and Corson, 1970]. A single straight wire carrying a current generates a magnetic field whose magnitude contours are concentric cylinders varying in direct proportion to the current and inversely with the distance from the wire [Lorrain and Corson, 1970]. We shall call this magnetic field from a single wire a ''line-source monopole field'' because its magnitude is identical in shape and distance-dependance to the electric field from monopoles (i.e., point charges) integrated along an infinite power line[1]

For a power line consisting of several wires, the magnetic field is the vector sum of the fields from the individual wires. For a pair of wires carrying unequal currents in opposite directions, the magnetic field is predominately a line-source monopole field proportional to the ''net current,'' the difference between the currents in the two lines (taking proper account of the current phases). Although a two-wire line with ''balanced currents'' will have zero net current and zero line-source monopole field, it still generates a field that is proportional to the current and the separation between the two wires and inversely proportional to the *square* of the distance from the line. These fields can be constructed by integrating the two-lobed fields from perpendicular point-source magnetic dipoles spread evenly along the power line, so we shall call them ''line-source dipole fields.''

For a straight power line with any number of wires, the magnetic field at any point can be expressed by a multipole expansion in cylindrical coordinates, which is a power series for the inverse of the perpendicular distance R to the line [Kaune and Zaffanella, 1992]. For R large relative to the wire spacing, the magnetic field is usually given accurately by the first non-zero term of the power series. Using the multipole expansion, the field's root-mean-squared (RMS) magnitude to a good approximation is:

$$B(R) = \left(\frac{\mu_0}{2\pi}\right)\frac{M_n}{R^n} \qquad (1)$$

where μ_0 is the magnetic permeability of air, and the magnetic line-source multipole M_n is either the RMS net current ($n = 1$) or the RMS magnitude of the line-source dipole vector ($n = 2$). Because Eq. (1) gives RMS magnetic fields, this model applies rigorously to the multiple-frequency fields generated by most power line.

The line-source dipole field is the dominant term in the multipole expansion for power lines that do not have grounded neutral wires for the return current. In this category are high-voltage transmission lines and

[1]The line-source monopole magnetic field is constructed by integrating point magnetic dipoles oriented parallel to the power line. Because these parallel magnetic dipoles have zero angular momentum perpendicular to the power line's axis, they function collectively as a monopole in cylindrical coordinates, which explains the congruity in the cross-sections of the field contors for line-source magnetic dipoles and electric monopoles integrated over a line.

some primary distribution lines (which carry power at intermediate voltage from a substation to a pole transformer). Without grounding along these lines, the currents at any location must be balanced by conservation of charge. On the other hand, lines with grounded neutrals will generally have unbalanced currents. In U.S. distribution systems, most primary lines and secondary distribution lines (which deliver power at 220 V to consumers) have neutrals grounded at frequent intervals and, therefore, should generate predominately line-source monopole fields. Because the Los Angeles utilities often use primary lines without neutrals, some primary lines in this area are expected to be line-source dipoles while others will be line-source monopoles.

To generalize, the RMS magnitude of the magnetic field from any power line can be modeled as either a line-source monopole field in a multipole expansion if the line has a neutral, or a line-source dipole otherwise. Based on the work of Wertheimer and Leeper [1979, 1982] and Kaune et al. [1987], we postulate that the line multipoles M_n in Eq. (1) may be modeled as empirical ''source functions'' S_n of wiring configuration variables such as the line's voltage, number of wires, capacity to carry current, etc.

The other important sources of residential magnetic fields are ground currents and electric appliances. ''Ground currents'' are created by unbalanced currents in the electric lines leading to a house, and consist of the net currents which are carried back to the distribution system through the earth, water pipes, TV cables, and other paths of least resistance. Ground currents are also line-source monopoles, but the locations of the conductors carrying ground currents within the home and the current magnitudes are unknown without complex measurements [Zaffanella, 1993]. The fields from ground current, therefore, cannot be modeled from the Los Angeles data using formulas derived from the Biot-Savart law. However, wiring configurations of neighborhood electrical lines can clearly have some effect on a home's ground currents and should be put into the model with an empirical source function S_0 that is independent of the distances from the home to the power lines. Appliance fields, however, should have no relation to wire configuration, and are represented only by a constant term in the model.

The magnetic fields in a home are, therefore, the vector sum of fields from a number of sources. The RMS magnitude of the superimposed fields from several sources around a house could in principle be calculated if one knew their phases and directions, in addition to their magnitudes. Because only the magnitudes are generally available, Kaune suggested that an expectation value for the total field could be computed by the ''random phase, random direction'' approximation [Kaune et al., 1987; Kaune, 1993]. In this approach, an average for the total field is estimated by integrating the vector sum over all possible phases and directions for the contributing fields. Thus, the expected RMS magnitude for the magnetic field in home h can be derived from the magnitudes generated by each wiring feature f:

$$B_h = \sqrt{\sum_f B_f^2} \tag{2}$$

These physical principles suggest a specific mathematical form for the relationship between magnetic fields at any point in the home and the wiring characteristics:

$$B_h^2 = \sum_f \left(\frac{S_{f1}}{R_{hf}}\right)^2 + \sum_f \left(\frac{S_{f2}}{R_{hf}^2}\right)^2 + \sum_f \left(S_{f0}\right)^2 \tag{3}$$

where R_{hf} are distances from power lines to the child's bedroom, and S_{fn} are the empirical source functions for different wiring features f: transmission lines and primaries with no neutrals ($n = 2$), primaries with neutrals and secondary lines ($n = 1$), and ground currents ($n = 0$). Because the source terms S_{fn} are RMS quantities, they must be non-negative functions of the wiring variables.

We, therefore, have a semiempirical model consistent with the Biot-Savart law for predicting magnetic fields from distances to power lines and the source functions S_n for line currents and ground currents. To obtain these source functions, we used regression modeling to fit Eq. (3) to the magnetic fields measurements and wiring data collected in the Los Angeles study of childhood leukemia.

METHODS

Data Collection

Wiring data and EMF measurements were obtained as part of the Los Angeles study of childhood leukemia, which was described in detail by London et al. [1991]. The study population was 646 children, half with leukemia and half without. Each child's residential history was obtained by interviewing a parent.

We obtained permission to take electric and magnetic field measurements at 318 homes where subjects had lived the longest. As part of these meaurements [London et al., 1991; Peters et al., 1991], the ELF magnetic field on the child's bedroom floor was monitored for 24 h with either an IREQ dosimeter (Institut de Recherche de Hydro-Quebec, Montreal, Canada) or an EMDEX (Electric Power Research Institute, Palo Alto, CA). These monitors record the RMS components in the x, y, and z directions with ELF filters at preset sampling intervals (10 s for the EMDEX and 50 s for the IREQ). With each sample, the RMS vector magnitude of the ELF magnetic field is calculated as the resultant of the three orthogonal components. For our model, exposures were summarized by the geometric mean of the RMS magnetic field magnitudes over 24 h. After excluding three unreliable measurements, estimates of the 24 h mean were available for a total of 315 homes, which is the data set used for the regression modeling.

Information on wiring configurations was also obtained for the subject's home where measurements were taken, as well as for all other subject homes we could locate in southern California (709 residences total). As illustrated in Figure 1, "field maps" were drawn to record neighboring high-voltage transmission lines, primary distribution lines, secondary distribution lines, and service drops (lines from the pole to the building). The field technician also recorded the type of residence (single-family house, apartment, etc.) and its main construction material (wood, stucco, etc.). Following the WL code [Wertheimer and Leeper, 1982], the field maps recorded all relevant wiring features within a 140 ft (43.4 m) distance from the outer walls of subject residences. Transmission lines beyond this radius were also recorded. Each field map

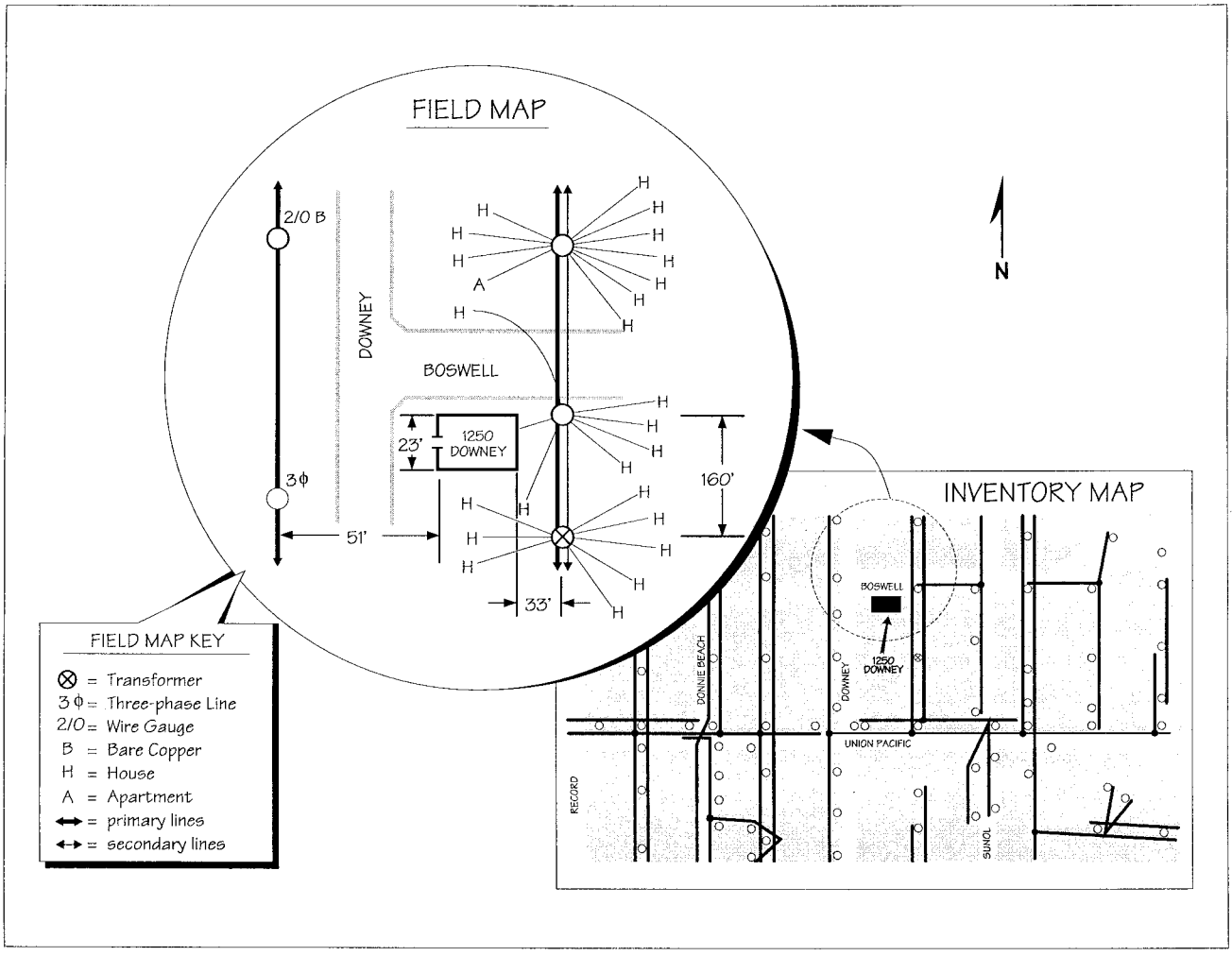

Fig. 1. Artist's rendering of the field map drawn by a study technician and the inventory map obtained from the utility for a residence in Los Angeles County. The inventory maps also have extensive notations (not shown) on line voltages, wire gauge, transformer capacity, etc. (1 ft = 0.305 m).

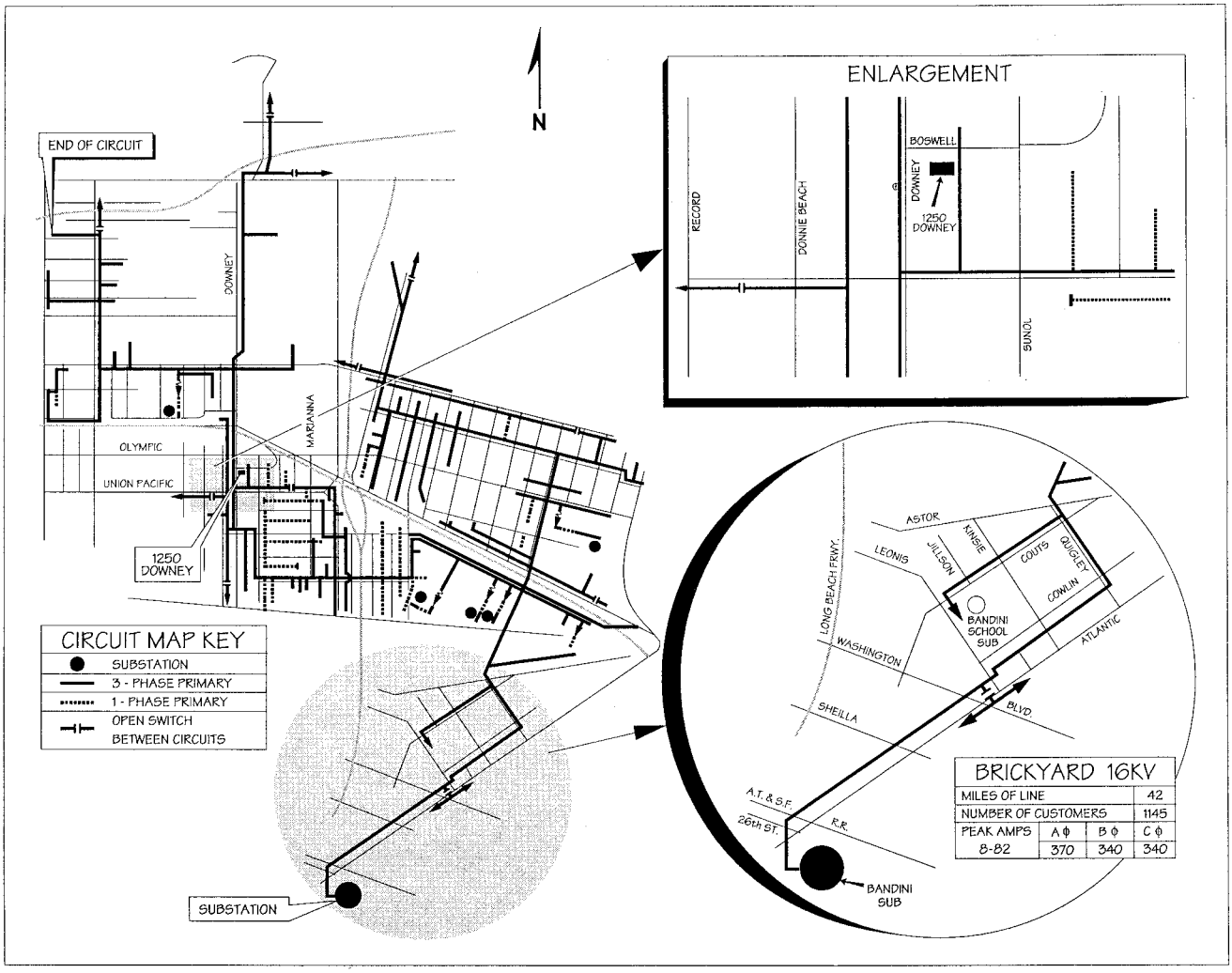

Fig. 2. Artist's rendering of the map of one primary circuit obtained from the utility for the same residence as depicted in Figure 1.

also noted the residence's width, depth (when accessible), and the horizontal distance from the building to one adjacent electric line, measured with a surveying wheel (Fig. 1). With apartment buildings, the location of the subject's unit was also drawn on the field map when that information could be recalled during the phone interview. From local utility companies, a scale map of all distribution wiring (the "inventory map," Fig. 1) and maps of each complete primary line ("circuit maps," Fig. 2) were obtained for each home.

Wiring data from the field map and the utility maps were transcribed onto a computerized scaled map of each residence by using the *Facility Mapping System for AutoCAD* (Facility Mapping Systems, Inc., Mill Valley, CA). To locate each feature exactly, the poles for each electric line were traced from the utility's inventory map (Fig. 1), and then the subject's house or apartment was drawn onto the AutoCAD map from the measurements recorded on the field map. For each line passing the residence, the perpendicular distance to the center of the living unit was then calculated from the AutoCAD map. Where a line stopped short of the residence, the shortest distance from the home to the line's "end-pole" was calculated, and the end-pole variable was set equal to one. All wiring features (lines, poles, and transformers) were assigned a series of "attributes" (distance to the home, wire material, transformer capacity, number of service drops, etc.) whose values were taken from the field and utility maps. For the example in Figure 1, attributes were recorded for the two primary lines, the secondary line, the transformer, and the five poles recorded on the field map. An illustrated coding book [Bowman, 1990] provided procedures for determining unambiguous values for these attributes from the wiring maps. After

the initial coding, each AutoCAD map was reviewed by others to ensure accuracy and consistency in coding the wiring configurations.

From the computerized map, an AutoCAD program extracted the attribute data for all wiring features inside a circle centered on the subject's living unit (house, apartment, townhouse, etc.). The extraction radius was the 140 ft distance specified by the WL code plus the measured width of the residence. If a subject's apartment had not been located exactly by the field technician, the width in the radius formula is half the street frontage of the whole building, and the extraction circle is centered in the middle of the building. By including the building's size in the radius, the AutoCAD data extraction approximates the WL code, which considers electric lines within 140 ft of the home's exterior.

TABLE 1. Wiring Configuration Variables: Definitions and Statistics for Los Angeles County Utilities

Type of source	Variable name	Definition (units)	Mean or Proportion[a]	
			DWP ($n = 96$)	SCE ($n = 178$)
Transmission line	Number	Number of lines per home	0.00	0.20
	Distance	(ft)[h]	—	135
	Voltage	(kV)	—	136
	Type	0 = subtransmission, 1 = hi voltage	—	43%
Primary line	Number	Number of lines per house	1.61	1.64
	Distance	(ft)	62	60
	Ampacity	(A)	185	212
	Peak current	(A)	N.A.	249
	Voltage	Operating voltage (kV)	4.8	9.3
	Endpole[b]	1 = endpole before line passes home, 0 = other	13%	12%
	Location	1 = overhead, 0 = underground	96%	96%
	Branches[c]	Proportion downstream	30%	34%
	Neutral	1 = neutral, 0 = no neutral	0%	53%
	Phases	1	0%	22%
		2	41%	35%
		3	59%	43%
	Customers	Number served by primary circuit	N.A.	473
Secondary line	Number	Number of lines per house	1.55	1.66
	Distance	(ft)	58	58
	Endpole[b]	1 = endpole before line passes home, 0 = other	30%	26%
	First span	1 = no upstream drops[d], 0 = other	41%	44%
	Location	1 = overhead, 0 = underground	93%	94%
	Triplex	1 = spun triplex[e], 0 = other	93%	89%
	Two-wire	1 = two-wire, 0 = other	1%	5%
Ground currents	Transformers	Number of transformers	1.25	1.36
		Unbanked transformer[f] capacity (kVA)	20.84	12.00
	Drops	Total direct drops[g]	3.64	4.24
		Total upstream drops[f]	1.94	1.63
		Total downstream drops[f]	2.32	2.07
		Commercial line drops[g]	0.78	0.66
		Industrial drops	0.02	0.03

[a]DWP, Department of Water and Power, City of Los Angeles; SCE, Southern California Edison; N.A., not applicable. Wiring statistics are evaluated inside a circle centered on each subject's residence with a radius of 140 ft plus a correction factor for the building's size.
[b]A line with an endpole does not pass the subject's residence, either because it terminates or bends away from the home.
[c]Branches: lines branching off a primary circuit as it goes from the substation to the residence (upstream branches) and on to the circuit's furthest extent (downstream).
[d] Upstream/downstream drops: line drops from an unbanked secondary line that passes the subject's residence, going either toward the transformer (upstream) or away (downstream).
[e]Spun triplex: secondary lines with two phases and a neutral twisted together.
[f] Banked/unbanked transformers: where a secondary line receives power from two or more poles, the transformers are banked.
[g]Direct/line drops: service drops originating either from a pole with a transformer (direct) or from the secondary line at another pole or between poles (line).
[h]1 ft = 0.305 m.

The wiring data extracted by these procedures are summarized by the statistics in Table 1. Parameters such as a primary's proportion of downstream branches and ampacity (current-carrying capacity) had to be derived from the information on the field and utility maps. The ampacity of primary lines near the residence was obtained from published tables [Kurtz and Shoemaker, 1986] as a function of the wire gauge and material (copper, aluminum or steel-reinforced aluminum), data we obtained from the utility maps (Fig. 1).

For the regression modeling, a computer program created a database of wiring attributes for each residence. Each electric line around the residence was described by its distance to the child's bedroom and such attributes as voltage, ampacity, and the number of "phases" (wires that carry voltage). To estimate the direct distance R between each electric line and the child's bedroom, the horizontal distance D from the building's center was determined from the AutoCAD map. The line's vertical distance H above a first-floor bedroom was assumed to be 25 ft for overhead secondary lines, 30 ft for primaries, 40 ft for subtransmission lines, 50 ft for high-voltage transmission lines, and 10 ft for underground lines (1 ft = 0.305 m). These values assume that the child's bedroom is on the first floor, which is generally the case in Los Angeles County. The direct distance R used in the wire configuration model (Eq. [3]) is then calculated as the resultant of the estimated horizontal and vertical distances: $R = \sqrt{D^2 + H^2}$.

Wiring attributes thought to contribute to ground currents are summed for all wiring features within the extraction radius. The ground current variables include the number of residential, commercial, and industrial service drops, the total power capacity of all transformers, and the number of banked and unbanked transformers ("banked" transformers, in our definition, provide power to the same secondary line from more than one pole). These wiring configuration variables, together with the 24-h measurements and information on the residence's structure, completed the data set for the regression modeling.

Finally, the five-category wire code of Wertheimer and Leeper [1982] was determined from the wiring data by a second computer algorithm. The WL code for a home is based on the type of lines, their horizontal distance from the home, and other wire attributes such as the number and thickness of primary phases. To determine the wire thickness objectively, we used the ampacity derived from the map data. Kaune et al. [1987] determined that "thick" primary lines in the WL code have an ampacity greater than 280 A, so the computer program determined whether each primary was thick or thin from its wiring data.

Regression Modeling

Although electromagnetic theory suggests much about the functional form of the regression model (Eq. [3]), the source functions S_{fn} are unspecified beyond the condition that as RMS vector magnitudes, they should be non-negative. Therefore, we chose to model them by nonlinear regression with the wiring data. The non-negative requirement plus the log-normal measurement data suggested a log-linear source function for the power lines:

$$S_{fn} = \exp\left(\beta_{0n} + \sum_{i>0} \beta_{in}(w_{fi} - \bar{w}_i)\right) \qquad (4)$$

where w_{fi} denotes the wiring variable i for line f, $\bar{w}_i$ is the mean value of the variable over all such lines, and β_{in} is the corresponding regression coefficient. The wiring variables w_{fi} are centered around their means to reduce correlations among the βs. For ground currents, a linear function of the wiring characteristics: $S_0 = \beta_{00} + \sum_i \beta_{i0}(w_i - \bar{w}_i)$ (with the constraint $S_0 \geq 0$ in the regression) seemed more appropriate, because that is how fields from different sources combine in the random phase approximation.

The regression parameters β_{in} were chosen to optimize the fit between the measured magnetic fields B_h and the predictions of Eq. (3). To design a nonlinear regression procedure, we first inspected the distribution of measurements over time within each house and of 24-h means between houses. Both were well characterized by lognormal distributions with standard deviations that were roughly proportional to the mean. We, therefore, used iteratively reweighted least squares to fit a lognormal model for the measured geometric mean fields B_h with logarithmic residual variances σ_h^2 that could vary between houses, i.e.,

$$WSS(\boldsymbol{\alpha}, \boldsymbol{\beta}) = \sum_h \frac{[\ln B_h - \ln \hat{B}_h(\boldsymbol{\beta})]^2}{2\sigma_h^2(\boldsymbol{\alpha}, \hat{B}_h)} \qquad (5)$$

where $\hat{B}_h(\boldsymbol{\beta})$ is the predicted field given by Eq. (3) and the residual variances are modeled as

$$\sigma_h^2(\boldsymbol{\alpha}, \hat{B}_h) = \exp[\alpha_0 + \alpha_1 \ln(\hat{B}_h) + \alpha_2 \ln^2(\hat{B}_h) + \alpha_3 \ln(GSD_h)] \qquad (6)$$

where GSD_h is the geometric standard deviation of the measurements over the 24-h period of measurement.

A Pascal program was written to fit the model, using Newton's method with numerical derivatives to

minimize Eq. (5) with respect to each component of $\boldsymbol{\beta}$ one at a time, treating the residual variances (Eq. [6]) as fixed. After each cycle, the $\boldsymbol{\alpha}$ parameters were estimated, holding the $\hat{B}_h(\boldsymbol{\beta})$ fixed. This ''quasi-likelihood'' process [McCullagh and Nelder, 1989] continued until all variables had converged. From the candidate variables in Table 1, the model's covariates were selected by a stepwise procedure, adding terms to the model that made significant ($p < .05$) contributions and deleting variables that later became nonsignificant.

Because there was some risk of overfitting the model, we then did a cross-validation by using the jackknife technique [Miller, 1974]. For each residence, the model in its final form was refitted to the database with that home omitted. Then, we computed the correlation between the observed magnetic field for each residence and the prediction from the model fit to all remaining homes. This jackknife correlation is less sensitive to outliers and is designed to estimate the predictive value of the model in a new data set.

RESULTS

Table 1 gives mean values of wiring characteristics for the two major utilities serving the study area—the City of Los Angeles Department of Water and Power (DWP) and Southern California Edison (SCE). The major difference between their wiring practices is that DWP has no neutrals on their primary lines (i.e., delta-connected primaries), whereas 53% of SCE primary lines carry neutrals (wye-connected). In addition, DWP distribution lines are grounded only at substations and the houses, while the neutrals on SCE lines are grounded at regular intervals (multigrounding). The peak current on a primary line at its substation and the numbers of customers served were only recorded on the SCE circuit maps (Fig. 2).

In the Los Angeles data, overhead power lines clearly had an impact on the magnetic field measurements. With overhead primaries, the geometric mean fields averaged 0.72 mG for homes with no lines within 140 ft ($n = 28$), 0.95 mG for homes with one line ($n = 159$), 1.05 mG with two lines ($n = 66$), and 1.39 mG with three or more lines ($n = 37$). With transmission lines, the measured fields showed a weak trend: 1.26 mG in the homes within 140 ft of a line ($n = 22$), 1.05 mG with a line at a greater distance ($n = 30$), and 0.98 mG with no transmission line. With secondary lines, the overall means actually declined: 1.72 mG in homes with no lines within 140 ft ($n = 14$), 1.01 mG with one ($n = 158$), and 0.93 mG with two or more lines ($n = 118$).

The 4% of primary lines that were underground had no effect on the residential fields (correlation = −0.05). Because the measured fields did not depend on the distance and other features of underground lines, they were not included in the regression analysis. Magnetic fields in homes with only underground lines

TABLE 2. Fitted Prediction Models by Utility (Jackknife Standard Errors)

Type of source	Variable name	Regression coefficient[a] (standard error)		
		DWP	SCE	Pooled
Transmission lines ($n = 2$)	Intercept	—	7.07 (1.00)	6.73 (0.59)
Primary neutral lines ($n = 1$)	Intercept	—	3.37 (0.10)	3.20 (0.15)
	Phases	—	0.27 (0.11)	—
	Peak current	—	−0.003 (0.001)	—
Primary non-neutral lines ($n = 2$)	Intercept	6.03 (0.32)	4.54 (0.11)	5.16 (0.19)
	Phases	2.11 (0.26)	0.78 (0.23)	2.68 (0.01)
	Ampacity	—	0.006 (0.001)	—
Secondary lines ($n = 1$)	Intercept	2.51 (0.15)	2.11 (0.20)	0.46 (1.37)
	Two-wire	—	—	2.33 (0.60)
	Endpole	−0.54 (0.32)	—	—
Ground currents ($n = 0$)	Intercept	0.46 (0.06)	0.35 (0.04)	0.46 (0.03)
	Transformers	−0.18 (0.06)	—	−0.07 (0.03)
	Total direct drops	−0.04 (0.02)	—	—
	Upstream drops	—	—	−0.02 (0.01)
	Downstream drops	0.11 (0.02)	—	—
	Commercial line drops	—	—	0.07 (0.02)
Residual variance	Intercept	0.02 (0.20)	0.92 (0.11)	0.37 (0.10)
	ln(predicted)	0.66 (0.55)	−0.37 (0.24)	−0.16 (0.25)
	$\ln^2$(predicted)	−0.18 (0.13)	−1.38 (0.40)	−0.50 (0.38)
	ln(GSD measured)	1.24 (0.73)	1.97 (0.06)	1.31 (0.11)

[a]DWP, Department of Water and Power; SCE, Southern California Edison; GSD, geometric standard deviation.

in their neighborhood are modeled by the mean fields measured in such homes.

Table 2 provides the regression coefficients for the best fitting models for DWP and SCE and for all utilities pooled (including 14 houses served by other companies). The best fit was achieved by separate models for each utility, which is not surprising in light of their different wiring practices. Table 3 lists the functional forms of the separate utility models for the magnetic fields B_f from the different wiring features. The functions in Table 3 incorporate all our assumptions about the multipole expansion (Eq. 1), the source terms (Eq. 4), and the vertical height of the lines, as well as the parameters in Table 2 and the variable means in Table 1.

For the DWP model, transmission lines made no contribution because none were adjacent to the homes with measurements. Primary lines made only a dipole contribution (because neutral lines are not used by that utility). The number of phases significantly modified the dipole source term with three-phase lines producing fields eight times larger than two-phase lines. The secondary line contribution was lowered by a factor of 0.58 if the home was served from an endpole. This endpole effect is expected because such lines do not carry current past the house, so the fringe field at the end of the line should fall off more rapidly than the model predicts. With ground currents, the field was increased by the number of downstream service drops, and decreased by transformers and ''direct drops,'' which come directly from the transformer's pole. Neither the type of residence (single family house, apartment, etc.) nor construction material entered into the DWP model or the other two models described below. This result is surprising because the Swedish model of transmission line fields did not agree with spot measurements as well in apartments as in single-family homes [Feychting et al., 1996].

Of these significant variables in the DWP model, the WL code also uses the number of phases and endpole status. Moreover, WL's ''first-span secondary'' is related to the number of downstream service

TABLE 3. Separate Utility Models for the Magnetic Fields B_f From Each Wiring Feature f as a Function of the Horizontal Distance D From the Line*

Wiring feature	DWP model	SCE model
Transmission lines (line-source dipoles)	None	$B_f[\text{mG}] = \dfrac{1176}{50^2 + D[\text{ft}]^2}$
Primary lines (line-source dipoles)	$B_f[\text{mG}] = \dfrac{416\,K_{\text{ph}}}{30^2 + D[\text{ft}]^2}$	$B_f[\text{mG}] = \dfrac{94.0\,K_{\text{ph}}K_{\text{amp}}}{30^2 + D[\text{ft}]^2}$
Phase factor		
2 phases	$K_{\text{ph}} = 0.29$	$K_{\text{ph}} = 0.84$
3 phases	$= 2.38$	$= 1.84$
Ampacity factor		$K_{\text{amp}} = \exp\{0.006(\text{amp[A]} - 213)\}$
Primary lines (line-source monopoles)	None	$B_f[\text{mG}] = \dfrac{29.1\,K_{\text{ph}}K_{\text{peak}}}{\sqrt{30^2 + D[\text{ft}]^2}}$
Phase factor		
1 phase		$K_{\text{ph}} = 0.72$
2 phases		$= 0.94$
3 phases		$= 1.23$
Peak current factor		$K_{\text{peak}} = \exp\{-0.003(\text{peak[A]} - 249)\}$
Secondary lines (line-source monopoles)	$B_f[\text{mG}] = \dfrac{14.47\,K_{\text{endpole}}}{\sqrt{25^2 + D[\text{ft}]^2}}$	$B_f[\text{mG}] = \dfrac{8.25}{\sqrt{25^2 + D[\text{ft}]^2}}$
	$K_{\text{endpole}} = 0.58$ if home is beyond endpole $= 1$ otherwise	

Ground currents	$B_f[\text{mG}] = 0.58 - 0.18\ \text{X}\ - 0.04\,\text{TDD} + 0.11\,\text{DD}$
	where X = # transformers
	TDD = # total direct drops
	DD = # downstream drops
		$B_f[\text{mG}] = 0.35$

*DWP, Department of Water and Power; SCE, Southern California Edison. Parameter units are not shown, but they can be deduced from the formulas by dimensional analysis.

drops, i.e. drops away from the transformer pole. The only new variables in the DWP model are the number of transformers and direct drops. The impact of these two features on ground currents has not been investigated, but they could plausibly divert neutral return currents from home grounding paths, explaining their negative parameters in the model.

For the SCE model, transmission lines had the strongest source term (1176 mG at 1 ft from the wire). On the ground floor of the child's home, however, this term did not make a very substantial contribution to predicted fields because line-source dipole fields ($n = 2$) fall off rapidly with distance and the lines are assumed to be 50 ft up. Both line-source monopole and dipole terms for primary lines were modified by the number of phases, although less than for DWP. The model predicts that the line-source monopole term decreases with peak currents and the dipole term increases with ampacity. The source terms for secondary lines and ground currents were not modified by any wiring variable.

Compared with the WL scheme, the only new variables in the SCE model are the primary's ampacity at the residence and its peak current measured at the substation, the two variables in our data most directly related to the current passing by the home. The ampacity of a primary near the residence is directly related to the thick or thin primaries in the WL code. Because magnetic fields increase with current, the positive contribution from primary's ampacity agrees with EMF principles, but the negative contribution from the peak current of the primary circuit at the substation seemingly contradicts them, the only aspect of these models to do so.

In the model with all utilities pooled (Table 2), transmission lines were again the strongest source term, but primary lines made the most important contributions to the predicted fields for most houses. Line-source dipole primaries are no longer modified by the number of phases. The average source term for secondary lines was 10 times higher for separate two-wire line than for spun triplex lines. Ground currents contributed an average of 0.46 mG and were positively related to the number of commercial line drops, negatively related to the number of transformers in the area and the number of upstream drops. The only new variables are commercial service drops from secondary lines and the number of upstream drops (a factor in WL's first-span secondary variable). The pooled model no longer contains several important variables in the separate utility models: phases for the line-source monopole primaries, ampacity for the dipole primaries, endpole status for secondaries, and the number of downstream drops. Overall, the pooled model does not agree with EMF principles and the WL code as well as the separate utility models, probably a reflection of the different distribution systems forced into the same model.

We used the separate utility models to calculate the magnetic field contributions from the different sources at all residences for which we have wiring data (Table 4). Our model predicts that magnetic fields from power lines (0.48 mG median, for example, with SCE) are larger than those from ground currents (0.23 mG SCE median). Among power lines, primaries with neutrals are the largest source (0.50 mG SCE median), followed by secondaries (0.07 mG), primaries with no neutral (0.04 mG), and transmission lines (0.01 mG). When the two utilities with their different distribution systems are compared, the modeled magnetic fields are surprisingly similar (median 0.69 mG for DWP and 0.53 mG SCE), and the median magnetic fields measured in a subset of homes are nearly identical (0.63 vs 0.61 mG). According to our model, the high fields from SCE's primary lines with neutrals (0.50 mG median) is matched by stronger contributions from DWP's secondaries (0.17 mG DWP vs. 0.07 mG SCE) and ground currents (0.31 vs. 0.23 mG).

For validating our model's predictions, an important data source on residential magnetic fields is EPRI's survey of 1000 homes from 25 U.S. utilities [Zaffanella, 1993]. This survey reports primarily the median magnetic field over a 24-h period, which closely approximates the geometric mean used in our analysis. This survey shows that electrical distribution and transmission wiring, plus the associated ground currents, are the foremost sources of magnetic fields away from electrical appliances. Both the EPRI survey and the wiring models find (1) household magnetic fields from power lines are greater than from ground currents, and (2) fields from overhead lines are greater than underground lines (Table 4). In agreement with the separate-utility models, data from the EPRI survey give positive correlations between the log-transformed median fields and the number of primary phases ($r = 0.33$–0.98 for neutral lines and 0.16–0.35 for non-neutrals, depending on the presence of secondaries). On the other hand, transmission lines are the source of the largest fields in the EPRI survey (median 0.90 mG), but are negligible in our study population (0.01 mG with SCE). Therefore, our models may be doing well with distribution lines and ground currents, but underestimating contributions from transmission lines.

We compared the predictive ability of these models with that of the WL code and an earlier regression model developed by Kaune et al. [1987]. The Kaune model's predictions from the Los Angeles wiring data were nonsignificantly negatively correlated

TABLE 4. Magnetic Field Contributions by Source (Separate Utility Models) Compared With the EPRI Survey (Zaffanella, 1993) and the Brain Tumor Study (Preston-Martin et al., 1996)

Source	*n*	24-h Geometric mean field (mG)	
		Median	95th percentile
Los Angeles Department of Water and Power			
All power lines	233	0.45	1.25
Transmission lines	0	—	—
Overhead distribution lines			
Primaries, no neutrals ($n = 2$)	202	0.04	0.92
Secondaries	210	0.17	0.48
Ground currents	235	0.31	0.92
Modeled magnetic field	235	0.69	1.36
Measured field (24-h GM)	97	0.63	4.18
Southern California Edison			
All power lines	442	0.48	1.47
Transmission lines	70	0.01	0.38
Overhead distribution lines			
Primaries with neutrals ($n = 1$)	222	0.50	1.46
Primaries, no neutrals ($n = 2$)	196	0.01	0.86
Secondaries	395	0.07	0.23
Ground currents	442	0.23	0.35
Modeled magnetic field	442	0.53	1.48
Measured field (24-h GM)	180	0.61	4.38
Los Angeles County brain tumor study[a]			
Measured field (24-h median)	260	0.52	3.58
EPRI survey[a]			
All power lines	991	0.40	2.00
Transmission lines	20	0.90	10.30
Underground lines	242	0.30	1.30
Ground currents	990	0.10	1.20
Modeled magnetic field	986	0.50	2.60
Measured field (average spot)	982	0.50	2.60

[a]The brain tumor and EPRI surveys reported the 24-h median magnetic field.

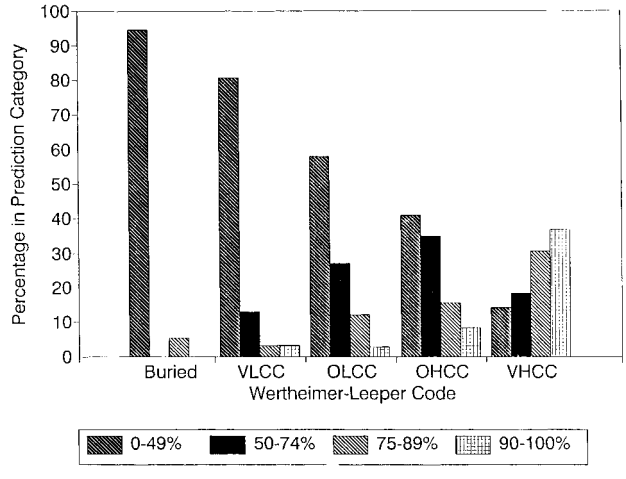

Fig. 3. Relationship of the Wertheimer-Leeper wire codes to the magnetic field predictions (pooled model), given as the percentage of homes in the exposure categories used in the epidemiologic analysis [Thomas et al. 1999]. The category boundaries are percentiles of the predicted field distribution for the controls. VLCC, very low current configuration; OLCC, ordinary low current configuration; OHCC, ordinary high current configuration, VHCC, very high current configuration.

with indoor fields [results not shown, see Jiang, 1992; Peters et al., 1994 for details] and were not pursued further. The WL codes for our data set are compared with our model and the measured fields, using percentiles of the utility-specific predictions in Figures 3 and 4 and correlations among the log-transformed exposure factors in Table 5. (For the correlation calculation, each WL code is assigned the corresponding geometric mean of the measured fields for homes in that category.)

It is clear that the WL code and our predicted values have some relationship (overall correlation 0.43 by using the utility-specific model). However, the prediction equations provides a better fit to the measured values than does the WL code ($r = 0.40$ vs. 0.27), even after applying the jackknife technique to the correlation with predicted values (the crude correlation was $r = 0.45$). Agreement with the measured fields was better with the DWP than the SCE model ($r = 0.47$ vs. 0.37), reflecting a mixture of wiring practices within the SCE system. The correlation with measurements is consistently better for the

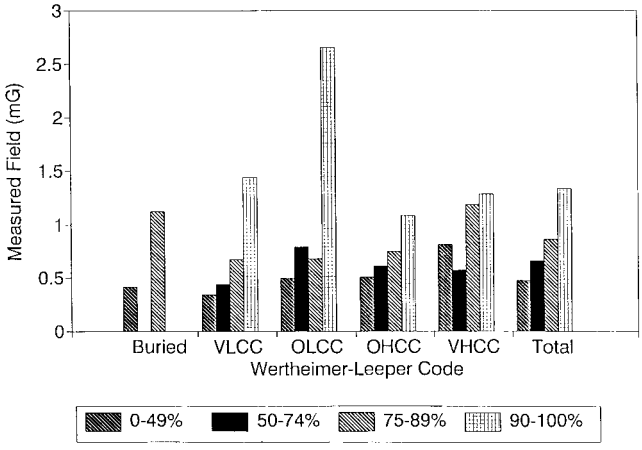

Fig. 4. Mean magnetic fields measurements for homes grouped by wire codes and predicted fields from the pooled model (with categories defined by percentiles of the exposure distribution). VLCC, very low current configuration; OLCC, ordinary low current configuration; OHCC, ordinary high current configuration, VHCC, very high current configuration.

separate models ($r = 0.40$) than for the pooled model ($r = 0.35$). The utility-specific models, therefore, are preferred over the pooled model because they have more variables in agreement with EMF theory as well as being empirically superior.

DISCUSSION

The results of the magnetic field modeling suggest that it is possible to improve upon the WL code for predicting residential magnetic fields from electrical wiring, at least for the two major utilities in Los Angeles County. The 24-h area measurements in the Los Angeles data correlate better with the predicted fields than with the WL code (Table 5).

The improvements over the WL code are due to (1) a regression model that fitted wiring data to magnetic field measurements taken inside the home, (2) a functional form for the model derived in part from physical principles, (3) including all the lines around the home in predicted indoor fields, (4) more wiring information collected from field observations and the utility maps, and (5) separate models for each utility with their different wiring practices. Of course, the better fit with measurements could come simply from a multivariate model's ability to exploit chance variations in the data. However, improvements due to random factors should be removed from the correlations in Table 5 by the jackknife cross-validation technique.

The functional form of our model and most wiring variables introduced by the regression modeling are plausible from the viewpoint of EMF theory, particularly for the separate utility models. However, the peak current of a primary line at its substation was retained as a variable in the SCE model even though its negative coefficient is difficult to explain physically. Although this decision made our model fit the measurements better, the model is a little less plausible as a predictor of magnetic fields from power lines. Another way to improve the model is suggested by the EPRI survey data [Zaffanella, 1993]. For primary lines with neutrals, the predominant field source in the nationwide survey was net currents (R^{-1}) for median field less than 1.6 mG, and balanced currents (R^{-2}) for

TABLE 5. Jackknifed Pearson Correlations Between Wertheimer-Leeper Code and Predicted and Measured Magnetic Fields (Log Scale), by Utility Company

Parameter	WL code	Predictions		Measurements (geometric mean)
		Pooled	Separate	
All Utilities				
WL code	1.00			
Predictions—pooled model	0.35	1.00		
Predictions—separate model	0.43	0.72	1.00	
Measurements (geometric mean)	0.27	0.35	0.40	1.00
Department of Water and Power				
WL code	1.00			
Predictions—pooled model	0.37	1.00		
Predictions—separate model	0.50	0.72	1.00	
Measurements (geometric mean)	0.26	0.35	0.47	1.00
Southern California Edison				
WL code	1.00			
Predictions—pooled model	0.32	1.00		
Predictions—separate model	0.39	0.76	1.00	
Measurements (geometric mean)	0.26	0.33	0.37	1.00

higher fields. Thus, a more accurate model should have both line-source monopole and dipole fields for primary lines with neutrals.

One possible advantage, which is shared by our model and the WL code, is the long-term stability of wiring configuration data. Many have suggested that the WL code, therefore, is better than contemporaneous measurements as a predictor of historical magnetic field exposures. However, the evidence on this point is mixed, particularly for children. Kheifets et al. [1997] reviewed the literature on wire codes and measurements and concluded that "wire codes are not superior (and perhaps inferior) to contemporary measurements in predicting prior exposures." This conclusion was based primarily on a large study with 396 adults wearing EMDEXs at home [Bracken et al., 1994] and discounted the agreement between wire codes and personal measurements with children in smaller pilot studies [Kaune and Zaffanella, 1994; Koontz and Dietrich 1994]. Based on this literature, our model's ability to predict long-term exposures cannot be assumed from the stability of wiring data, and should be tested by measurements.

The magnetic fields from Los Angeles sources are generally predicted to be higher than those in EPRI's national survey, particularly at the 95th percentile (Table 4). This systematic elevation in our predicted magnetic fields can be traced to the higher 24-h magnetic field monitored at the site of the child's bed in our study (95th percentile of 4.17 mG), which are definitely higher than the spot measurements averaged over the entire residence in the EPRI survey (95th percentile of 2.60 mG). As shown in Figure 5, this same elevation of the monitored magnetic fields occurs with our spot measurements taken in the center of the room (95th percentile of 2.78 mG at normal power). In a subsequent Los Angeles study of childhood brain tumors [Preston-Martin et al., 1996], the 24-h median fields in the child's bedroom has a 95th percentile of 3.58 mG, which lie between the values from the childhood leukemia study and both sets of spot measurements (Fig. 5).

The most likely explanation for the elevated magnetic fields in the childhood leukemia data is the placement of the monitors at the site of the child's bed while most spot measurements were taken in the room's center. Calibrations and other comparisons between the monitors and the spot meters preclude significant instrumental bias [London et al., 1991; Peters et al., 1991]. While the instrument placement may account for part of the elevated 24 h fields, the monitoring data from the 1991 leukemia study is also higher than the results from the 1994 brain tumor study (Table 4; Fig. 5).

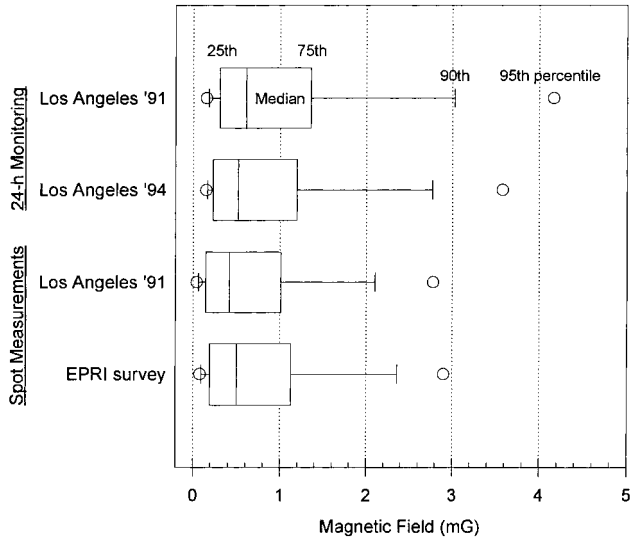

Fig. 5. Magnetic field distributions from 24 h monitoring at the site of the child's bed and from the average of spot measurements throughout the residence, comparing our Los Angeles data [London et al., 1991] with another Los Angeles study [Preston-Martin et al., 1996] and EPRI's survey of U.S. residences [Zaffanella, 1993].

A source of bias in the 1991 childhood leukemia study is the possibility that the 24-h monitoring occasionally measured elevated fields from nearby appliances, particularly electric clocks beside the bed. Such appliances are an artifact in the exposure assessment because they were not necessarily present when the subject originally slept there. Therefore, the brain tumor study systematically avoided placing the monitor next to localized sources of magnetic fields in the vicinity of the child's bed [Preston-Martin et al., 1996]. For these reasons, the 24-h magnetic fields from the leukemia study are generally higher than other studies of residential magnetic fields designed to avoid the localized magnetic fields from appliances. The same conclusion should apply to our wire configuration models, which are based on the measurements from the leukemia study.

As predictors of contemporaneous measurements, the wiring configuration models are better than the WL code but still not very accurate, e.g., the correlation for the most accurate DWP model is 0.47. This substantial imprecision reflects the limitations of estimating residential magnetic fields based on wiring features and distances observable from public space outside the home. With this constraint, the model can make consistent exposure predictions for all residences where the subjects lived without permission from the home owner, thereby increasing the number of subjects in the epidemiologic analysis and reducing selection

bias. However, the constraint on data collection also requires some crude approximations in the model, such as assuming the child's bedroom is in the center of the living unit or neglecting the distance from ground currents to the bedroom. The impact of the resulting exposure assessment errors on risk estimates will be discussed more in the companion paper [Thomas et al., 1999].

In retrospect, a number of improvements in our data collection would have made the exposure model better. Of course, the monitor should have always been located away from local magnetic field sources in the bedroom. Furthermore, the elevation of the lines relative to the bedroom turned out to be an important parameter in the model and should have been measured or estimated for all lines. After taking measurements in Los Angeles, Leeper [1986–1989] recommended improving the model's predictive power by taking spot measurements of the magnetic fields over neighborhood water pipes to estimate ground currents. Data on metal or plastic water mains serving the residence might also predict ground current effects. Because air conditioning is a big factor in Los Angeles electricity usage, Leeper suggested that the ambient temperature on the day of monitoring might help the model correct for day-to-day variations from the long-term mean magnetic field exposure. (Day-of-the week was tested in the regression model and was not predictive.)

Before using our model in other utility service areas, it is important that its predictions be validated with comparable measurements. It may not predict magnetic field exposures as well as it did in Los Angeles because wiring practices differ substantially between utility companies. Neither the WL code, which was developed in Denver, nor the regression model of Seattle wiring [Kaune et al., 1987] has predicted fields well in other areas. Future epidemiologic studies outside Los Angeles will therefore need to take in-home measurements in a representative sample of homes.

Lastly, we observe that this methodology can be used to develop wiring configuration models of long-term exposure for other magnetic field metrics. For example, Thomas et al. [1994] report an association between childhood leukemia risks in the Los Angeles data and measurements of temporal variability metrics like the first-order correlation in the ELF magnetic field. However, the association with the measured temporal variability metrics was weaker than the association with the WL code. An obvious explanation for this familiar paradox is that the WL code is a better predictor of long-term exposures to the temporal variability metrics. To test this supposition, a wiring configuration model for the first-order autocorrelation and any other temporal variability metric could be developed by using Eq. (3) with the 24-h measurements, the wiring configuration data, and the regression methods described above.

In this approach, we are assuming that our model applies to the temporal variability metrics like the autocorrelation as well as to the geometric mean field. Certainly the multipole expansion of the Biot-Savart law (Eq. [1]) is valid for instantaneous ELF magnetic fields originating from the electrical distribution system. The remaining question is whether the random-phase, random-direction approximation (Eq. [2]) applies to other metrics like the rate of change. This model assumption can be tested empirically with data sets like the EPRI survey [Zaffanella, 1993]. The wiring configuration model can theoretically be applied to more sophisticated exposure metrics such as the field's polarization or dB/dt (the predictor of induced body current). However, more complex metrics require more sophisticated instruments for EMF measurements in epidemiologic studies

CONCLUSIONS

We have developed a new model for residential ELF magnetic fields that only needs distance measurements and wiring configuration data from utility maps and field observations in the vicinity of the home. This model is empirically and theoretically superior to the Wertheimer-Leeper wire code as a surrogate for ELF magnetic field exposures in Los Angeles county. Empirically, the model predictions correlate better with measurements. Theoretically, the model's functional form is in agreement with electromagnetic principles, it incorporates new wiring features such as delta-connected primaries, and its parameters are determined by regression analysis against household measurements in the study region. As a predictor of long-term exposure, the quantitative model, like the WL code, depends only on distances and wiring data that are temporally more stable than 24-h measurements. The prediction model is also superior to measurements in epidemiologic analyses because gathering the input data does not require the homeowner's permission (although measurements are needed in a sample of residences for model validation). Thus, magnetic field risks estimated from the model's predictions are not as subject to selection bias as those from measurements.

The remaining question is whether the magnetic field exposures predicted by the model are associated with childhood leukemia risk. This question is addressed in the following paper [Thomas et al., 1999].

ACKNOWLEDGMENTS

We gratefully acknowledge the expert assistance of Leopoldo Herrara, Isabel Nader, Thomas Trauger, and William Lapworth with data collection and analysis. For generous assistance throughout this study, we are indebted to the Los Angeles Department of Water and Power and Southern California Edison, especially Kirby Holte, Ram Mukherji, and Jack Sahl.

REFERENCES

Bowman JD. 1990. Wire configuration rules. Unpublished protocol, Department of Preventive Medicine, University of Southern California.

Bracken TD, Rankin RF. 1994. The EMDEX project residential study. EPRI Report TR-104325. Palo Alto, CA: Electric Power Research Institute.

Feychting M, Kaune WT, Savitz DA, Ahlbom A. 1996. Estimating exposure in studies of residential magnetic-fields and cancer: importance of short-term variability, time-interval between diagnosis and measurement, and distance to power-line. Epidemiology 7:220–224.

Fulton JP, Cobb S, Preble L, et al. 1980. Electrical wiring configurations and childhood leukemia in Rhode Island. Am J Epidemiol 11:292–296.

Jiang F. 1992. Regression modeling of residential magnetic field exposure from wiring configurations. Unpublished M.Sc. Thesis, Dept. of Preventive Medicine. Los Angeles, CA: University of Southern California.

Kaune WT. 1993. Introduction to power-frequency electric and magnetic fields. Environ Health Persp 101(Suppl 4):73–81.

Kaune WT, Zaffanella LE. 1992. Analysis of magnetic fields produced far from electric power lines. IEEE Trans Power Deliv 7:2082–2090.

Kaune WT, Zaffanella LE. 1994. Assessing historical exposure of children to power-frequency magnetic fields. J Exp Anal Environ Epidemiol 2:149–170.

Kaune WT, Stevens RG, Callahan NJ, et al. 1987. Residential magnetic and electric fields. Bioelectromagnetics 8:315–335.

Kheifets LI, Kavet R, Sussman SS. 1997. Wire codes, magnetic fields, and childhood cancer. Bioelectromagnetics 18:99–110.

Koontz MD, Dietrich FM. 1994. Variability and predictability of children's exposure to magnetic fields. J Exp Anal Environ Epidemiol 3:287–307.

Kurtz EB, Shoemaker TM. 1986. The lineman's and cableman's handbook, 7th edition. New York: McGraw-Hill.

Leeper E. 1986–1989. Letters to J. Bowman, unpublished.

Linet MS, Hatch EE, Kleineman RA, et al. 1997. Residential exposure to magnetic fields and acute lymphoblastic leukemia in children. N Engl J Med 337:1–7.

London SJ, Thomas DC, Bowman JD, et al. 1991. Exposure to residential electric and magnetic fields and risk of childhood leukemia. Am J Epidemiol 134:923–937.

Lorrain P, Corson DR. 1970. Electromagnetic fields and waves, 2nd edition. San Francisco: W.H. Freeman, pp 295–297, 319–321, 388.

McCullagh P, Nelder JA. 1989. Generalized linear models, Section 10.2. London: Chapman and Hall.

Miller RG. 1974. The jackknife—a review. Biometrika 61:1–15.

National Research Council. 1996. Possible health effects of exposure to residential electric and magnetic fields. Washington, DC: National Academy Press.

Peters JM, Thomas DC, Bowman JD, Sobel E, London SJ, Cheng TC. 1991. Exposure to residential electric and magnetic fields and risk of childhood leukemia (Interim Report). Palo Alto, CA: Electric Power Research Institute, (Report EN-7464).

Peters JM, Thomas DC, Bowman JD, Sobel E, London SJ, Cheng TC. 1995. Exposure to residential electric and magnetic fields and risk of childhood leukemia. EPRI Report TR-104528. Palo Alto, CA: Electric Power Research Institute.

Preston-Martin S, Navidi W, Thomas DC, Lee P, Bowman JD. 1996. Los Angeles study of residential electromagnetic fields and childhood brain tumors. Am J Epidemiol 143: 105–119.

Savitz DA, Wachtel H, Barnes FA, et al. 1988. Case-control study of childhood cancer and exposure to 60-Hz magnetic fields. Am J Epidemiol 128:21–38.

Thomas DC, Jiang L, London S, Bowman JD, Peters J. 1994. Temporal variability in residential magnetic fields and risk of childhood leukemia. USC Biostatistics Division Technical Report #97. Los Angeles, CA: University of Southern California.

Thomas DC, Bowman JD, Liangzhong J, Feng J, Peters JM. 1999. Residential magnetic fields predicted from wiring configurations: II. Relationship to childhood leukemia. Bioelectromagnetics 20:414–422.

Wertheimer N, Leeper E. 1979. Electrical wiring configurations and childhood cancer. Am J Epidemiol 109:273–284.

Wertheimer N, Leeper E. 1982. Adult cancer related to electrical wires near the home. Int J Epidemiol 11: 345–355.

Zaffanella LE. 1993. Survey of residential magnetic field sources. EPRI Report TR-102759. Palo Alto, CA: Electric Power Research Institute.